**Journal of Electrical, Marine and Its Application Technology** **Vol. …...., No. …….**
**ISSN xxxxxx** **Publication Periode**

# Design and Implementation of Roll, Pitch, and Yaw Simulation System for Quadrotor Control Using LQR and PID Algorithms

**M. Alief Framuja[1], Fortunaviaza Habib Ainudin[2], Anggara Trisna Nugraha[3]**
[1,2,3] Marine Electrical Engineering, Shipbuilding Institute of Polytechnic Surabaya
[1] mframuja@student.ppns.ac.id , [2] fhabib@student.ppns.ac.id ,[3] anggaranugraha@ppns.ac.id

## Abstract

The performance of a control system is often evaluated based on its ability to achieve minimal settling time and rise time. However, an optimal control system must also exhibit rapid and precise rotational responses to external commands, ensuring dynamic stability and responsiveness. This study focuses on the design and implementation of a DC motor speed control system using optimal control techniques to enhance settling time, rise time, and overall system performance. The research employs two prominent methods: the Proportional-Integral-Derivative (PID) controller and the Linear Quadratic Regulator (LQR) algorithm. Optimization in the LQR method is achieved by tuning the Q and R matrices to derive the optimal gain feedback (K) that minimizes the quadratic cost function. The process begins with mathematical modeling of the DC motor within the PID controller framework, enabling seamless integration into the LQR calculation. The simulation and implementation of the control system are conducted in MATLAB Simulink, allowing for comprehensive analysis of the system's dynamic responses. The results demonstrate the comparative advantages of each control method, highlighting the practical implications for applications requiring precise rotational speed control. This research contributes to advancements in control engineering by providing a systematic approach to optimizing DC motor performance, with potential applications in robotics, automation, and aerospace systems. Future work includes experimental validation and exploration of adaptive methods for further enhancement of control robustness.

Keywords: proportional-integral-derivative (PID), Linear Quadratic Regulator (LQR), Pitch

## 1. Introduction

Quadrotors, a subclass of multicopters, are equipped with four propellers whose rotational speeds can be independently adjusted to generate roll, pitch, and yaw movements. These capabilities make quadrotors highly versatile for various applications, including aerial surveillance, autonomous delivery, and scientific exploration (Zakariz, Praska, Nugraha, & Phasinam, 2022). The control of these movements, however, remains a critical challenge, requiring advanced algorithms to ensure stability, precision, and responsiveness.

Previous research has explored different control methods for optimizing quadrotor motion. Hoffmann et al. (Industri, 2016) employed the Extended Kalman Filter (EKF) to estimate speed and position measurements using GPS while stabilizing altitude and attitude with the Linear Quadratic Regulator (LQR). Similarly, Gibiansky (Achmad & Nugraha, 2022) (Liberty, 1972). demonstrated the effectiveness of the Proportional-Integral-Derivative (PID) controller in achieving stable flight dynamics. Despite these advancements, comparative studies combining LQR and PID for roll, pitch, and yaw control in a unified simulation framework are limited.

This research aims to address this gap by designing and implementing a simulation system for quadrotor motion control using LQR and PID algorithms. The study focuses on evaluating the performance of these controllers in terms of dynamic stability, response time, and robustness to disturbances. The findings are expected to contribute to the development of more efficient and reliable control systems for quadrotors, thereby advancing their applications in engineering and technology domains (Nugraha et al., 2022b).

## 2. Material and methods

### 2.1. Quadrotor System

Quadrotor can move in any direction due to the force generated from the rotation of 4 propellers (Hoffmann, Huang, Waslander, & Tomlin, 2011) . The propeller on the quadrotor consists of 2 pairs of propellers with opposite rotational directions as shown in Fig. 1 (Bresciani, 2008) (Informatics et al., 2014).

DOI xxxxxx

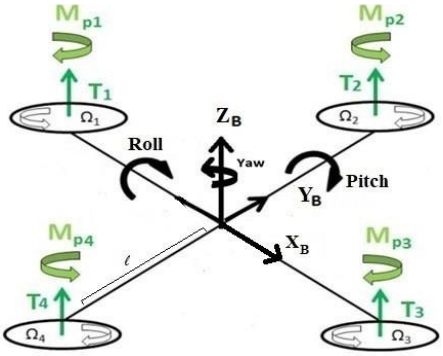


**Figure 1.** Quadrotor motion mechanism.

The first pair of propellers consists of propellers 1 and 3, while the second pair consists of propellers 2 and 4. Pitch motion is achieved by increasing the rotational speed of propeller 1 (Ω1) and decreasing the rotational speed of propeller 3 (Ω3), or vice versa. Roll motion occurs by increasing the rotational speed of propeller 2 (Ω2) and decreasing the rotational speed of propeller 4 (Ω4), or vice versa. Yaw motion is produced by increasing the rotational speed of the first propeller pair and decreasing the rotational speed of the second pair, or the reverse. Roll motion results in a change in the angle $\phi$ (phi), pitch motion results in a change in the angle $\theta$ (theta), and yaw motion leads to a change in the angle $\psi$ (psi) (García Carrillo, Dzul López, Lozano, & Pégard, 2013) (Nugraha, As'ad, & Abdullayev, 2022). The mathematical model that describes the rotational motion of the quadrotor is presented in equations (Bresciani, 2008) (Ivannuri, Fahmi, & Nugraha, 2022) (Gibiansky, 2012).

$$\Phi(t)=\frac{\left(\Omega_2^2(t)-\Omega_4^2(t)\right)K_T l}{I_{xx}}$$

$$\theta(t)=\frac{\left(\Omega_1^2(t)-\Omega_3^2(t)\right)K_T l}{I_{yy}}$$

$$\Psi(t)=\frac{\left(\Omega_1^2(t)-\Omega_2^2(t)+\Omega_3^2(t)-\Omega_4^3(t)\right)K_M}{I_{zz}}$$

KT represents the aerodynamic force constant, $KM$ is the aerodynamic moment constant, and $l$ denotes the quadrotor's arm length. $I$XX, $Iyy$, and $Izz$ are the moments of inertia around the $XB$, $YB$, and $ZB$ axes, respectively, corresponding to the rotational motion around those axes. The angle $\phi$ is obtained through the integral of the angular acceleration $\dot{\phi}$, while the angle $\theta$ is derived by integrating the angular acceleration $\dot{\theta}$. Similarly, the angle $\psi$ is determined from the integral of the angular acceleration $\dot{\psi}$ (Asri et al., 2022) (Nugraha et al., 2022c). The physical parameters of the quadrotor, including $KT$, $KM$, $l$, $Ixx$, $Iyy$, and $Izz$, are specified in Table 1 (Hoffmann, Huang, Waslander, & Tomlin, 2011).

**Table 1.** Quadrotor physical parameters.

| Parameter | Value | Unit |
|---|---|---|
| $Ixx$ | $7{,}5 \times 10^{-3}$ | Kg.$m^2$ |
| $Iyy$ | $7{,}5 \times 10^{-3}$ | Kg.$m^2$ |
| $Izz$ | $1{,}3 \times 10^{-2}$ | Kg.$m^2$ |
| $l$ | 0,23 | m |
| $K_T$ | $3{,}1 \times 10^{-5}$ | Kg.m.$rad^{-2}$ |
| $K_M$ | $7{,}5 \times 10^{-7}$ | Kg.$m^2$.$rad^{-2}$ |

### 2.2. Controller

A. Linear Quadratic Regulator Control

The optimization method with LQR aims to determine the control signal that will move the state of a system from the initial state $X(t0)$ to a final state $X(t)$ which will minimize the cost function (Domingues, 2009). The cost function ($JLQR$) in question is the time integral of the quadratic form in the $X$ vector and the $U$ vector (Nugraha et al., 2022a) .

The principle of using the LQR method is to obtain the optimal control signal from the state feedback according to equation (Nugraha et al., 2022a).

$$U = K_{LQR} X$$

$$K_{LQR} = R^{-1} B^T P$$

$KLQR$ is the state feedback gain, $P$ is the solution of the Riccati algebraic equation (Nugraha, Priyambodo, & Sarena, 2022). The solution of the Riccati algebraic equation is calculated based on equation

$$A^T P + PA - PBR^{-1} B^T P + Q = 0$$

B. PID Control with Tuning Method Ziegler-Nichols Tuning Method

$$U(t) = K_P \left( e(t) + \frac{1}{\tau_i} \int_0^t e(t)\, dt + \frac{T_d\, de(t)}{dt} \right)$$

The application of the Ziegler-Nichols tuning method aims to determine the values of the parameters $Kp$, $Ti$, and $Td$ in equation (Asri et al., 2022). The Ziegler-Nichols tuning method can be applied in two ways: s-curve response analysis and oscillation response analysis. Application of s-curve response analysis by giving step input to a plant without feedback (open loop). If the response curve to the input step is shaped like the letter s then response curve analysis can be applied and vice versa. Since the quadrotor does not produce an s-shaped response curve, oscillation response analysis is applied. The application of oscillatory response analysis only uses proportional control action on the close loop system. The value of $K$P must be increased from 0 to its critical value, causing the system output to be an oscillating signal with constant amplitude (Bouabdallah, Noth, Siegwart, & Siegwan, 2004). Analysis of the oscillatory response requires critical gain ($Kcr$) and critical period ($Pcr$) parameters. The value of $Kcr$ is the critical value of $K$P when the system starts to produce an oscillating signal with constant amplitude (Nugraha, Ramadhan, & Shiddiq, 2022). The value of $Pcr$ is obtained by measuring the period of the oscillating signal from peak to peak as shown in Fig. 2. The parameters $Kcr$ and $Pcr$ are used to calculate the values of $K$, $T$, and $T$ based on Table 2 (Arrosida, 2016).

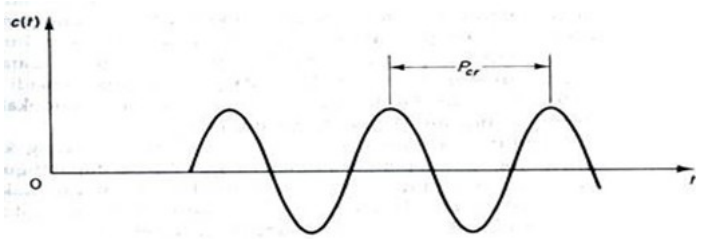


**Figure 1.** Measurement of the Pcr value of the oscillating signal.

**Table 2.** Determination of Kp, Ti, and Td values in the Ziegler-Nichols tuning method based on oscillation response

| Control Type | $K_p$ | $T_i$ | $T_d$ |
|---|---|---|---|
| **P** | $0{,}5K_{cr}$ | - | - |
| **PI** | $0{,}45K_{cr}$ | $\frac{1}{1{,}2} P_{cr}$ | - |
| **PID** | $0{,}6K_{cr}$ | $0{,}5P_{cr}$ | $0{,}125P_{cr}$ |

## 2.3. Methods

A. LQR Control Design on Quadrotor

In designing the LQR, it is essential to determine the value of $KLQR$. To do this, the $Q$ matrix and the $R$ matrix must first be determined through trial and error using the following steps:

- Create 10 different variations of the $Q$ matrix as shown in Table 3, while setting the $R$ matrix as the identity matrix. The $Q$ matrix that results in the system having the smallest rise time in its response will be chosen.

- Create 10 variations of the $R$ matrix as shown in Table 5, while the $Q$ matrix is selected from the variation that produces the smallest rise time. The $R$ matrix that leads to the system response with the smallest rise time will be chosen.

**Table 2.** Variation of Matix Q.

| No. | Matrix Q |
|---|---|
| 1 | $\begin{bmatrix} 20 & 0 & 0 & 0 & 0 & 0 \\ 0 & 1 & 0 & 0 & 0 & 0 \\ 0 & 0 & 20 & 0 & 0 & 0 \\ 0 & 0 & 0 & 1 & 0 & 0 \\ 0 & 0 & 0 & 0 & 20 & 0 \\ 0 & 0 & 0 & 0 & 0 & 1 \end{bmatrix}$ |
| 2 | $\begin{bmatrix} 20 & 0 & 0 & 0 & 0 & 0 \\ 0 & 100 & 0 & 0 & 0 & 0 \\ 0 & 0 & 20 & 0 & 0 & 0 \\ 0 & 0 & 0 & 100 & 0 & 0 \\ 0 & 0 & 0 & 0 & 20 & 0 \\ 0 & 0 & 0 & 0 & 0 & 100 \end{bmatrix}$ |
| 3 | $\begin{bmatrix} 40 & 0 & 0 & 0 & 0 & 0 \\ 0 & 1 & 0 & 0 & 0 & 0 \\ 0 & 0 & 40 & 0 & 0 & 0 \\ 0 & 0 & 0 & 1 & 0 & 0 \\ 0 & 0 & 0 & 0 & 40 & 0 \\ 0 & 0 & 0 & 0 & 0 & 1 \end{bmatrix}$ |
| 4 | $\begin{bmatrix} 40 & 0 & 0 & 0 & 0 & 0 \\ 0 & 100 & 0 & 0 & 0 & 0 \\ 0 & 0 & 40 & 0 & 0 & 0 \\ 0 & 0 & 0 & 100 & 0 & 0 \\ 0 & 0 & 0 & 0 & 40 & 0 \\ 0 & 0 & 0 & 0 & 0 & 100 \end{bmatrix}$ |

5
$$\begin{bmatrix} 60 & 0 & 0 & 0 & 0 & 0 \\ 0 & 1 & 0 & 0 & 0 & 0 \\ 0 & 0 & 60 & 0 & 0 & 0 \\ 0 & 0 & 0 & 1 & 0 & 0 \\ 0 & 0 & 0 & 0 & 60 & 0 \\ 0 & 0 & 0 & 0 & 0 & 1 \end{bmatrix}$$

6
$$\begin{bmatrix} 60 & 0 & 0 & 0 & 0 & 0 \\ 0 & 100 & 0 & 0 & 0 & 0 \\ 0 & 0 & 60 & 0 & 0 & 0 \\ 0 & 0 & 0 & 100 & 0 & 0 \\ 0 & 0 & 0 & 0 & 60 & 0 \\ 0 & 0 & 0 & 0 & 0 & 100 \end{bmatrix}$$

7
$$\begin{bmatrix} 80 & 0 & 0 & 0 & 0 & 0 \\ 0 & 1 & 0 & 0 & 0 & 0 \\ 0 & 0 & 80 & 0 & 0 & 0 \\ 0 & 0 & 0 & 1 & 0 & 0 \\ 0 & 0 & 0 & 0 & 80 & 0 \\ 0 & 0 & 0 & 0 & 0 & 1 \end{bmatrix}$$

8
$$\begin{bmatrix} 80 & 0 & 0 & 0 & 0 & 0 \\ 0 & 100 & 0 & 0 & 0 & 0 \\ 0 & 0 & 80 & 0 & 0 & 0 \\ 0 & 0 & 0 & 100 & 0 & 0 \\ 0 & 0 & 0 & 0 & 80 & 0 \\ 0 & 0 & 0 & 0 & 0 & 100 \end{bmatrix}$$

9
$$\begin{bmatrix} 300 & 0 & 0 & 0 & 0 & 0 \\ 0 & 1 & 0 & 0 & 0 & 0 \\ 0 & 0 & 300 & 0 & 0 & 0 \\ 0 & 0 & 0 & 1 & 0 & 0 \\ 0 & 0 & 0 & 0 & 300 & 0 \\ 0 & 0 & 0 & 0 & 0 & 1 \end{bmatrix}$$

| | |
|---|---|
| 10 | $\begin{bmatrix} 300 & 0 & 0 & 0 & 0 & 0 \\ 0 & 100 & 0 & 0 & 0 & 0 \\ 0 & 0 & 300 & 0 & 0 & 0 \\ 0 & 0 & 0 & 100 & 0 & 0 \\ 0 & 0 & 0 & 0 & 300 & 0 \\ 0 & 0 & 0 & 0 & 0 & 100 \end{bmatrix}$ |

The results of the system response to the variation of matrix $Q$ for unit step input are shown in Fig. 3 while the response specification in the form of rise time is shown in Table 4.

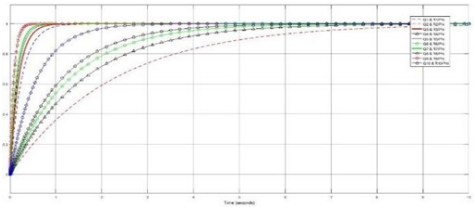

**Figure 1.** LQR response to variation of Q matrix.

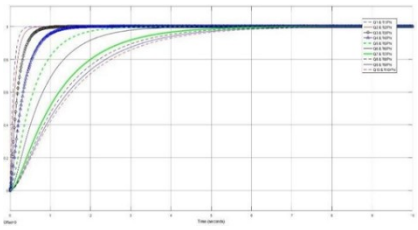

**Figure 4.** LQR response to variation of R matrix

**Table 4.** Rise time of matrix Q variation.

| No. | Variation of Matrix Q | Rise Time (milisecon) | | |
|---|---|---|---|---|
| | | Roll | Pitch | Yaw |
| **1** | Q1 | 534,042 | 534,042 | 483,066 |
| **2** | Q2 | 4614 | 4614 | 4610 |
| **3** | Q3 | 392,163 | 392,163 | 342,602 |
| **4** | Q4 | 3389 | 3389 | 3384 |
| **5** | Q5 | 328,152 | 328,152 | 279,122 |
| **6** | Q6 | 2783 | 2783 | 2777 |
| **7** | Q7 | 290,463 | 290,463 | 290,463 |
| **8** | Q8 | 2415 | 2415 | 2415 |
| **9** | Q9 | 170,783 | 170,783 | 127,67 |
| **10** | Q10 | 1253 | 1253 | 1247 |

Table 4 shows that the smallest rise time is caused by the variation of the 9th Q matrix (Q9). Table 4 shows that if the values of the 1st, 3rd, and 5th diagonal elements get bigger while the values of the 2nd, 4th, and 6th diagonal elements get smaller in the $Q$ matrix, the rise time gets smaller. The trial and error process is continued by making 10 variations of the $R$ matrix while the $Q$ matrix is selected from the 9th variation of the $Q$ matrix.

**Table 5.** Variation of matrix R.

| No. | Matrix R |
|---|---|
| 1 | $\begin{bmatrix} 1 & 0 & 0 \\ 0 & 1 & 0 \\ 0 & 0 & 1 \end{bmatrix}$ |

2 $$\begin{bmatrix} 10 & 0 & 0 \\ 0 & 10 & 0 \\ 0 & 0 & 10 \end{bmatrix}$$

3 $$\begin{bmatrix} 100 & 0 & 0 \\ 0 & 100 & 0 \\ 0 & 0 & 100 \end{bmatrix}$$

4 $$\begin{bmatrix} 1000 & 0 & 0 \\ 0 & 1000 & 0 \\ 0 & 0 & 1000 \end{bmatrix}$$

5 $$\begin{bmatrix} 10000 & 0 & 0 \\ 0 & 10000 & 0 \\ 0 & 0 & 10000 \end{bmatrix}$$

6 $$\begin{bmatrix} 40000 & 0 & 0 \\ 0 & 40000 & 0 \\ 0 & 0 & 40000 \end{bmatrix}$$

7 $$\begin{bmatrix} 200000 & 0 & 0 \\ 0 & 200000 & 0 \\ 0 & 0 & 200000 \end{bmatrix}$$

8 $$\begin{bmatrix} 300000 & 0 & 0 \\ 0 & 300000 & 0 \\ 0 & 0 & 300000 \end{bmatrix}$$

9 $$\begin{bmatrix} 400000 & 0 & 0 \\ 0 & 400000 & 0 \\ 0 & 0 & 400000 \end{bmatrix}$$

10 $$\begin{bmatrix} 500000 & 0 & 0 \\ 0 & 500000 & 0 \\ 0 & 0 & 500000 \end{bmatrix}$$

The results of the system response in roll, pitch, and yaw movements to variations in the $R$ matrix for unit step input are shown in Fig. 4 while the response specifications in the form of rise time are shown in Table 6.

**Table 6.** Rise time of matrix variation response R.

| No. | Variation of Matrix R | Rise Time (milisecon) | | |
|---|---|---|---|---|
| | | Roll | Pitch | Yaw |
| **1** | R1 | 170,323 | 170,323 | 126,813 |
| **2** | R2 | 242,024 | 242,024 | 144,229 |
| **3** | R3 | 390,079 | 390,079 | 209,482 |
| **4** | R4 | 668,92 | 668,92 | 340,405 |
| **5** | R5 | 1176 | 1176 | 596,511 |
| **6** | R6 | 1656 | 1656 | 824,491 |
| **7** | R7 | 2476 | 2476 | 1232 |
| **8** | R8 | 2733 | 2733 | 1362 |

| | | | | |
|---|---|---|---|---|
| **9** | R9 | 2934 | 2934 | 1462 |
| **10** | R10 | 3099 | 3099 | 1548 |

Table 5 shows that the smallest rise time is caused by variations from the $R$ to 1 (R1) matrix. Table 5 shows that the diagonal element in the $R$ matrix also has an effect when its value is smaller, the rise time is smaller. Based on the trial error results, it can be concluded that the variation of matrix $Q$ to 9 and matrix $R$ to 10 causes the system to respond quite well. The next step is to calculate the value of $P$, the results of which are shown in equation.

$$P=\begin{bmatrix} 44{,}3968 & 0{,}0439 & 0 & 0 & 0 & 0 \\ 0{,}0439 & 0{,}0011 & 0 & 0 & 0 & 0 \\ 0 & 0 & 44{,}3968 & 0{,}0439 & 0 & 0 \\ 0 & 0 & 0{,}0439 & 0{,}0011 & 0 & 0 \\ 0 & 0 & 0 & 0 & 43{,}3061 & 0{,}0175 \\ 0 & 0 & 0 & 0 & 0{,}0175 & 0{,}0004 \end{bmatrix} \quad (11)$$

The P value is used to calculate KLQR, the result of which is shown in equation (12).

$$K_{LQR}=\begin{bmatrix} 1346{,}1 & 33 & 0 & 0 & 0 & 0 \\ 0 & 0 & 1346{,}1 & 33 & 0 & 0 \\ 0 & 0 & 0 & 0 & 1346{,}1 & 32{,}2 \end{bmatrix} (12)$$

B. PID Control Design on Quadrotod

When simulated in Simulink for 103 seconds and the value of $Kcr$ is increased gradually until it reaches a value of 0.000005, the output always produces an oscillating signal while when the simulation is run for 108 seconds, the simulation results are shown in Fig. 5.

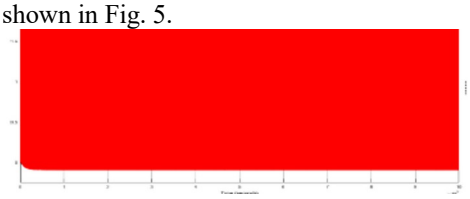

(a) Response of the close loop system on the roll unit when the $K_{cr}$ value is equal to 0.000004 for $10^8$ seconds.

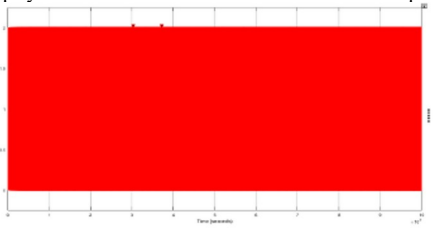

(b) close loop system response of the roll unit when the $K_{cr}$ value is equal to 0.000005 for $10^8$ seconds.

**Figure 2.** Close loop system response with controller. Proportional to the unit roll for $18^0$ seconds.

Fig. 5 shows an increase in amplitude in the simulation results when the $K_{cr}$ value is 0.000004 while when the $K_{cr}$ value is 0.000005 there is no increase in amplitude so that the Kcr value chosen is 0.000005. In the oscillation signal, the first peak appears at the 260th second while the second peak appears at the 760th second so that the Pcr value is :

$$P_{cr}=760-260=500$$

The next step is to calculate the $K_p$, $T_i$, and $T_d$ values for the PID roll based on Table 2.

$$K_p=0{,}6\times 0{,}000005=0{,}000003$$

$$T_i = 0{,}5 \times 500 = 250$$

$$T_d = 0{,}125 \times 500 = 62{,}5$$

The values of $K_p$, $T_i$, and $T_d$ are used to complete the PID roll design as shown in Figure 6.

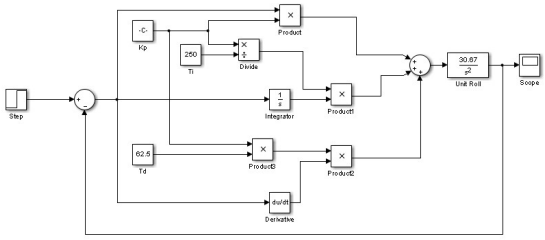


**Figure. 3.** Results of PID roll design.

- Pitch PID Design

When simulated in Simulink for 103 seconds and the value of $Kcr$ is increased gradually until it reaches 0.000005, it always outputs an oscillating signal while when the simulation is run for 108 seconds, the simulation results are identical to the unit roll in that there is an increase in amplitude in the simulation results when the value of $K_{cr}$ is 0.000004 while when the value of $K_{cr}$ is 0.000005 there is no increase in amplitude so the value of $K_{cr}$ chosen is 0.000005. In the oscillation signal, the first peak appears at the 260th second while the second peak appears at the 760th second so the value of $P_{cr}$ is :

$$P_{cr} = 760 - 260 = 500$$

The next step is to calculate the $K_p$, $T_i$, and $T_d$ values for the PID roll based on Table 2.

$$K_p = 0{,}6 \times 0{,}000005 = 0{,}000003$$

$$T_i = 0{,}5 \times 500 = 250$$

$$T_d = 0{,}125 \times 500 = 62{,}5$$

The values of Kp, Ti, and Td are used to complete the pitch PID design as shown in Figure 7.

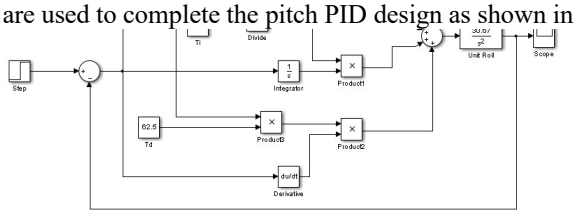


**Figure 4.** Deisgn result of pitch PID.

- Yaw PID Design

When simulated in Simulink for 500 seconds and the $Kcr$ value was increased gradually until it reached 0.000013, it always produced an oscillating signal as output while when the simulation was run for 108 seconds, it showed slightly different results from the roll unit where there was an increase in amplitude in the simulation results when the $Kcr$ value was 0.000012 while when the $Kcr$ value was 0.000013 there was no increase in amplitude in the simulation results so the $Kcr$ value chosen was 0.000013. The $Pcr$ value for the yaw PID was determined by measuring the period of the oscillation signal from peak to peak. When the $Kcr$ value of 0.000013 was simulated for 500 seconds, the simulation results showed an oscillation signal with the first peak

appearing at the 100th second and the second peak appearing at the 300th second, so the $Pcr$ value for the yaw PID was determined as follows:

$$P_{cr} = 300 - 100 = 200$$

The next step is to calculate the values of $K_p$, $T_i$, and $T_d$ based on Table 2.

$$K_p = 0{,}6 \times 0{,}000013 = 0{,}0000078$$

$$T_i = 0{,}5 \times 200 = 100$$

$$T_d = 0{,}125 \times 200 = 25$$

The values of $K_p$, $T_i$, and $T_d$ are used to complete the yaw PID design as shown in Figure 8.

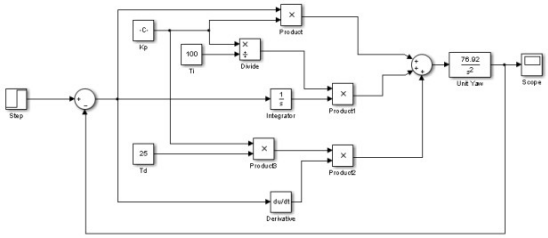


**Figure 5.** Design result of yaw PID.

## 3. Results and discussion

Tests were conducted by providing step input to change the angle from 0 radians to 0.8 radians. The first test was conducted to control roll motion. The LQR response is shown in Fig. 9 while the PID response is shown in Fig. 10. The response specifications of the LQR and PID in roll motion are shown in Table 7.

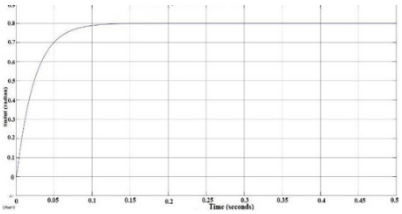

**Figure. 6.** LQR response in roll and pitch movements.

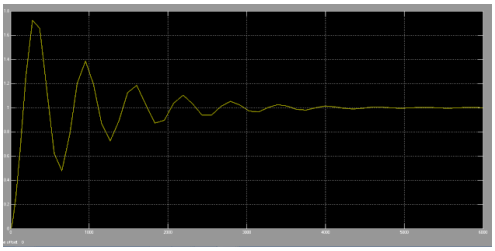

**Figure 10.** PID response in roll and pitch movements

**Table 7.** Response specifications of LQR and PID in roll and pitch movement

| Response Specification | LQR | PID |
|---|---|---|
| Rise time (miliseconds) | 50,611 | $109{,}81 \times 10^3$ |
| Overshoot (%) | 0,501 | 80,909 |
| Setling time (miliseconds) | 70,544 | $3372 \times 10$ |

The second test was conducted to control pitch motion. The LQR and PID responses show the pitch motion test results are identical to the roll motion test results. The third test was conducted to control yaw motion using LQR and PID. The LQR response in yaw motion is shown in Fig. 11 while the PID response is shown in Fig. 12. The response specifications of the LQR and PID in yaw motion are shown in Table 8.

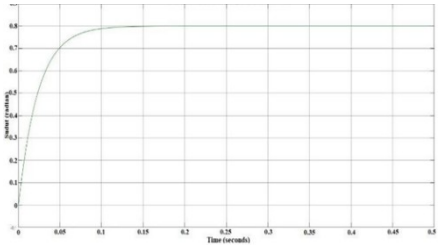

**Figure 11.** LQR response in yaw movements.

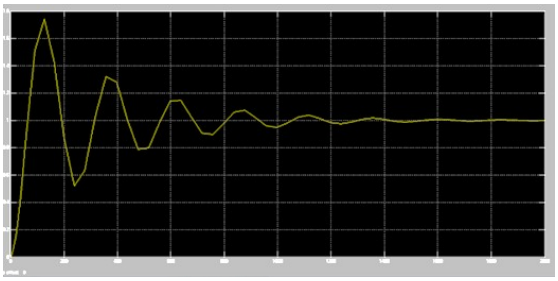

**Figure 12.** PID response in yaw movements

**Table 8.** Response specification of LQR and PID in yaw movements

| Response Specification | LQR | PID |
|---|---|---|
| Rise time (miliseconds) | 50,637 | $43{,}88 \times 10^3$ |
| Overshoot (%) | 0,501 | 77,679 |
| Setling time (miliseconds) | 70,625 | $1223 \times 10^3$ |

## 4. Conclusion

In conclusion, the results of this study demonstrate that the Linear Quadratic Regulator (LQR) control system provides superior performance in terms of dynamic response when compared to the Proportional-Integral-Derivative (PID) controller. Specifically, the LQR algorithm yields more precise control over roll, pitch, and yaw motions, making it a more robust choice for quadrotor stabilization in dynamic environments. However, while LQR proved to be effective in this simulation framework, the PID controller also offers advantages in simplicity and computational efficiency, particularly in scenarios with fewer system constraints.

For future work, it is recommended that the translational motion of the quadrotor, including forward and vertical movements, be explored in further depth. This would provide a more holistic approach to quadrotor control, as rotational and translational dynamics are interdependent. Additionally, the integration of optimization techniques, such as genetic algorithms, to fine-tune the control parameters for both LQR and PID controllers could enhance system performance. By adapting the control gains through optimization, the system could achieve more efficient and adaptable control strategies, improving the quadrotor's overall stability, responsiveness, and versatility in real-world applications.

**Credit authorship contribution statement**

**Author Name**: Conceptualization, Writing – review & editing. **Author Name**: Supervision, Writing – review & editing. **Author Name**: Conceptualization, Supervision, Writing – review & editing.

## References

T. Bresciani, “Modelling, Identification and Control of a Quadrotor Helicopter,” English, vol. 4, no. October, p. 213, 2008.

Ivannuri, Fahmi, and Anggara Trisna Nugraha. "Implementation Of Fuzzy Logic On Turbine Ventilators As Renewable Energy." Journal of Electronics, Electromedical Engineering, and Medical Informatics 4.3 (2022): 178-182.

F. T. Industri, "TUNING PARAMETER LINEAR QUADRATIC TRACKING TRACKING USING GENETIC ALGORITHM FOR," 2016.

Achmad, Irgi, and Anggara Trisna Nugraha. "Implementation of Voltage Stabilizers on Solar Cell System Using Buck-Boost Converter." Journal of Electronics, Electromedical Engineering, and Medical Informatics 4.3 (2022): 154-160.

G. M. Hoffmann, H. Huang, S. L. Waslander, and C. J. Tomlin, "Precision flight control for a multi-vehicle quadrotor helicopter testbed," Control Eng. Pract., vol. 19, no. 9, pp. 1023–1036, 2011.

Nugraha, Anggara Trisna, Reza Fardiyan As' ad, and Vugar Hacimahmud Abdullayev. "Design And Fabrication of Temperature and Humidity Stabilizer on Low Voltage Distribution Panel with PLC-Based Fuzzy Method to Prevent Excessive Temperature and Humidity on The Panel." Journal of Electronics, Electromedical Engineering, and Medical Informatics 4.3 (2022): 170-177.

A. Gibiansky, "Quadcopter Dynamics, Simulation, and Control Introduction Quadcopter Dynamics," pp. 1–18, 2012.

Asri, Purwidi, et al. "Desain Hybrid Panel Surya dan Generator Set pada Kapal Ikan Pesisir Selatan Jawa." Jurnal Inovtek Polbeng 12.1 (2022): 46-53.

J. Domingues, "Quadrotor prototype," Inst. Super Tec. Univ. Tec. …, no. October, p. 129, 2009.

Nugraha, Anggara Trisna, et al. "Brake Current Control System Modeling Using Linear Quadratic Regulator (LQR) and Proportional integral derivative (PID)." Indonesian Journal of Electronics, Electromedical Engineering, and Medical Informatics 4.2 (2022): 85-93.

H. Arrosida, "Perancangan Metode Kontrol LQR ( Linear Quadratic Regulator ) Sebagai Solusi Optimal Pengendalian Gerak Quadrotor," vol. 1, no. November, pp. 109–122, 2016.

Nugraha, Anggara Trisna, Dadang Priyambodo, and Sryang Tera Sarena. "Design A Battery Charger with Arduino Uno-Based for A Wind Energy Power Plant." JPSE (Journal of Physical Science and Engineering) 7.1 (2022): 23-38.

S. Bouabdallah, A. Noth, R. Siegwart, and R. Siegwan, "PID vs LQT control techniques applied to an indoor micro quadrotor," 2004 IEEE/RSJ Int. Conf. Intell. Robot. Syst. (IEEE Cat. No.04CH37566), vol. 3, pp. 2451–2456, 2004.

Nugraha, Anggara Trisna, Moch Fadhil Ramadhan, and Muhammad Jafar Shiddiq. "DISTRIBUTED PANEL-BASED FIRE ALARM DESIGN." JEEMECS (Journal of Electrical Engineering, Mechatronic and Computer Science) 5.1 (2022).

L. R. García Carrillo, A. E. Dzul López, R. Lozano, C. Pégard, and SpringerLink (Online service), "Quad Rotorcraft Control Vision-Based Hovering and Navigation," Adv. Ind. Control., p. XIX, 179 117 illus., 74 illus. in color., 2013

Zakariz, Naufal Praska, Anggara Trisna Nugraha, and Khongdet Phasinam. "The Effect of Inlet Notch Variations in Pico-hydro Power Plants with Experimental Methods to Obtain Optimal Turbine Speed." Journal of Electronics, Electromedical Engineering, and Medical Informatics 4.1 (2022): 35-41.

D. Informatics, A. Afis, A. Arisekola, and A. I. Street, "THE USE OF MATLAB IN THE SOLUTION OF LINEAR QUADRATIC REGULATOR (LQR) PROBLEMS," vol. 5, no. 4, pp. 15–32, 2014

Nugraha, Anggara Trisna, et al. "The Auxiliary Engine Lubricating Oil Pressure Monitoring System Based on Modbus Communication." Proceedings of the 2nd International Conference on Electronics, Biomedical Engineering, and Health Informatics. Springer, Singapore, 2022.

S. Liberty, Modern control engineering, vol. 17, no. 3. 1972.

Nugraha, Anggara Trisna, et al. "Battery Charger Design in a Renewable Energy Portable Power Plant Based on Arduino Uno R3." Proceedings of the 2nd International Conference on Electronics, Biomedical Engineering, and Health Informatics. Springer, Singapore, 2022.